Temperature-Induced Denaturation and Renaturation of Triosephosphate Isomerase from *Saccharomyces cerevisiae*: Evidence of Dimerization Coupled to Refolding of the Thermally Unfolded Protein[†]

Claudia G. Benítez-Cardoza, Arturo Rojo-Domínguez, and Andrés Hernández-Arana*

Área de Biofisicoquímica, Departamento de Química, Universidad Autónoma Metropolitana-Iztapalapa, Apartado Postal 55-534, Iztapalapa D.F. 09340, Mexico

Received March 14, 2001; Revised Manuscript Received May 21, 2001

ABSTRACT: The thermal denaturation of the dimeric enzyme triosephosphate isomerase (TIM) from *Saccharomyces cerevisiae* was studied by spectroscopic and calorimetric methods. At low protein concentration the structural transition proved to be reversible in thermal scannings conducted at a rate greater than 1.0 °C min^{-1}. Under these conditions, however, the denaturation−renaturation cycle exhibited marked hysteresis. The use of lower scanning rates lead to pronounced irreversibility. Kinetic studies indicated that denaturation of the enzyme likely consists of an initial first-order reaction that forms *thermally unfolded* (U) TIM, followed by irreversibility-inducing reactions which are probably linked to aggregation of the unfolded protein. As judged from CD measurements, U possesses residual secondary structure but lacks most of the tertiary interactions present in native TIM. Furthermore, the large increment in heat capacity upon denaturation suggests that extensive exposure of surface area occurs when U is formed. Above 63 °C, reactions leading to irreversibility were much slower than the unfolding process; as a result, U was sufficiently long-lived as to allow an investigation of its refolding kinetics. We found that U transforms into nativelike TIM through a second-order reaction in which association is coupled to the regain of secondary structure. The rate constants for unfolding and refolding of TIM displayed temperature dependences resembling those reported for monomeric proteins but with considerably larger activation enthalpies. Such large temperature dependences seem to be determinant for the occurrence of kinetically controlled transitions and thus constitute a simple explanation for the hysteresis observed in thermal scannings.

Triosephosphate isomerase (TIM)[1] is a dimeric enzyme formed by identical subunits of approximately 26 kDa each. Within each monomer, the polypeptide chain adopts a folding pattern based on an 8-fold repeat of a β-strand−loop−helix−loop motif, with the β-strands forming a barrel-like structure at the core of the molecule and the helices packing against the outer surface of the barrel (*1*). This conspicuous folding architecture, often called the TIM barrel, has been found in many different proteins with various functions (*2*). In dimeric TIM, the monomer−monomer interface is mainly formed by residues in loops 1, 3, and 4 of each subunit; loop 3, an especially long loop in the structure, projects from one subunit and fits into a cavity between loops 1 and 4 of the other subunit.

Studies on the renaturation kinetics of TIM from its monomers unfolded in guanidine hydrochloride (GuHCl) have demonstrated that the recovery of enzymatic activity is closely related to the occurrence of a bimolecular reaction (*3*, *4*); besides, it has been found that a unimolecular reaction takes place before dimer formation. Hence, the mechanism of TIM renaturation has usually been described as a sequential pathway in which folding of the monomer precedes the association step. However, the extent of structural consolidation in the "folded" monomer is currently unknown. Recently, it has been shown that the isomerase from *Saccharomyces cerevisiae* (yeast TIM) dissociates into partially folded monomers in the presence of moderate concentrations of GuHCl (*5*, *6*). Whereas this monomeric form of the protein retains significant secondary structure, it lacks the tertiary interactions that are characteristic of the native enzyme (*6*). As suggested by Morgan et al. (*6*), such a species could be related to the monomeric intermediate that participates in the association step of the renaturation pathway.

Regarding the thermal stability of TIM, studies of the heat denaturation of several wild-type TIMs, as well as a number of their mutants, have been carried out (*7*−*12*). In most instances, it has been found that the process is irreversible and linked to aggregation of the denatured protein. Mainfroid et al. (*12*), however, were able to perform equilibrium studies of human TIM denaturation in solutions of low protein concentration; the concentration dependence of thermal

[†] This work was supported in part by CONACYT, México (Convenio No. 400200-5-29124E) and TWAS (Grant 98-252 RG/CHE/LA). C.G.B.-C. was supported by CONACYT (94713).

* Address correspondence to this author: Fax, +52 (5) 804 46 66; e-mail, aha@xanum.uam.mx.

[1] Abbreviations: TIM, triosephosphate isomerase; CD, circular dichroism; DSC, differential scanning calorimetry; Tris, tris(hydroxymethyl)aminomethane; GuHCl, guanidine hydrochloride; TEA, triethanolamine; NADH, nicotinamide adenine dinucleotide, reduced form; α-GDH, α-glycerophosphate dehydrogenase.

10.1021/bi010528w CCC: $20.00
Published on Web 07/07/2001

transitions indicated that in this case denaturation is compatible with a two-state process involving the native dimer and the unfolded monomer as the only states populated at equilibrium. Nevertheless, neither the kinetics of the process nor the degree of unfolding reached upon denaturation has been investigated so far.

In the present work, we have shown that thermal scannings on a solution of yeast TIM give rise to fully reversible transitions when the enzyme is present in low concentration and the scanning rate is larger than 1.0 °C min^{-1}. However, under these conditions the denaturation−renaturation process is kinetically controlled, as evidenced by the marked hysteresis that displays. Because heat-denatured TIM is prone to aggregate, attempts to reach "equilibrium" transitions by decreasing the scanning rate conduce only to an increasing irreversibility. If denaturation is carried out at temperatures above 63.0 °C, a partially folded species is formed in a time short enough to avoid the occurrence of deleterious aggregation reactions. We were thus able to study the kinetics of refolding of such a species in a concentration range appropriate for detection of its far-UV circular dichroism (CD) signal. We have found that the refolding reaction obeys second-order kinetics and leads to the formation of dimeric, nativelike TIM. As far as we know, this is the first report on the renaturation of a TIM enzyme indicating that dimerization is coupled to the regain of a large amount of secondary structure.

MATERIALS AND METHODS

Materials. Two lots of yeast triosephosphate isomerase were used. One of them was purchased from Sigma (St. Louis, MO) and further purified in a monoQ HR 10/10 column installed in a fast-protein liquid chromatograph from Pharmacia (Piscataway, NJ). The sample was eluted by a linear gradient of 0−100 mM NaCl that was created with a buffer containing 10 mM triethanolamine (TEA), 1 mM ethylenediaminetetraacetate (EDTA), and 1 mM dithiothreitol, pH 8.0. The other lot of enzyme was produced and purified as described by Vázquez-Contreras et al. (*5*). The two lots showed similar enzymatic activities; their spectroscopic properties and denaturation profiles were essentially identical. However, commercial TIM was not able to refold upon thermal denaturation. The homogeneity of protein samples was checked by SDS−PAGE analysis. Concentrations of protein solutions were determined from their absorbances at 280 nm, using the absorption coefficient reported for yeast TIM [$A_{1cm}(1\%) = 10.0$ (*13*)]. Unless otherwise stated, further studies were carried out in a buffer solution of 50 mM tris(hydroxymethyl)aminomethane (Tris) adjusted to pH 8.5 (at 25 °C) with HCl. All reactants were of analytical grade. The water used was distilled and deionized.

Activity Assays. Enzymatic activity was determined by a coupled assay with α-glycerophosphate dehydrogenase (α-GDH), following NADH absorbance changes at 340 nm (*14*). Routine assays were made at 25.0 °C in 1.0 mL of 0.1 M TEA buffer (pH 7.4) containing 10 mM EDTA, 0.2 mM NADH, 10 μg mL^{-1} α-GDH, and 1.0 mM DL-glyceraldehyde 3-phosphate as substrate. The reaction was started by addition of 4 ng of TIM. Enzyme activity was also determined at 43.2 °C in 0.1 M Tris buffer, pH 8.5. Concentrations of the other substances present in the solution were the same as in standard assays, except for the coupling enzyme whose concentration was increased to 25 μg mL^{-1}. We checked that in the latter conditions both enzymes were stable enough to bring about a constant rate of reaction for a period of several minutes.

Differential Scanning Calorimetry. Calorimetric endotherms were obtained with a MicroCal MC-2 differential scanning calorimeter (MicroCal, Northampton, MA). Measurements were carried out in buffer solutions of pH 8.5 (0.05 M Tris) and pH 10.0 (0.05 M glycine), employing heating rates from 0.2 to 1.0 °C min^{-1}. The effect of protein concentration (in the 0.70−2.90 mg mL^{-1} range) on the endotherm was investigated at pH 8.5. A total pressure of 2.7 atm was applied with nitrogen gas to both cells in the calorimeter. Solutions were extensively dialyzed before measurements. Buffer−buffer tracings were recorded under the same conditions and subtracted from sample endotherms. All thermodynamic data are given per mole of dimeric protein (53.3 kDa), unless otherwise stated. The Origin software package (MicroCal) was used for data analysis including baseline subtraction and calculation of denaturation enthalpies (ΔH_{cal}).

Thermal Transitions Monitored by Circular Dichroism Spectroscopy. CD measurements were done in a JASCO J-715 spectropolarimeter (Jasco Inc., Easton, MD) equipped with a PTC-348WI Peltier-type cell holder for temperature control and magnetic stirring. Thermal denaturation transitions were followed by continuously monitoring ellipticity changes at a fixed wavelength of 220 nm, while the sample temperature was increased at constant rate. The range of heating rates was from 0.05 to 3.0 °C min^{-1}. Typically, TIM solutions of 0.010 mg mL^{-1} and 1.0 cm cells were used. Actual temperatures within the cell were registered with the external probe of the cell holder. Renaturation profiles were recorded after the denaturation transition had been completed; cooling rates were also controlled through the Peltier accessory. CD spectra were recorded by employing either 1.0 cm or 0.1 cm cells. Ellipticities are reported as mean residue ellipticity [θ].

Denaturation Kinetics. The kinetics of TIM denaturation was followed by changes in ellipticity at 220 nm. Cells of 1.0 cm path length were filled up to 98% of their total volume (3.0 mL) with the Tris buffer and allowed to equilibrate at the temperature of the experiment. Temperature within the cell was measured with the external probe of the Peltier accessory. The necessary amount of concentrated TIM solution was then injected to complete the cell volume. Samples were vigorously stirred to promote rapid mixing and temperature equilibration. Under these conditions the dead time of experiments was less than 10 s. Kinetic data were adjusted to a single exponential decay equation, $\theta_t = \theta_f + (\theta_0 - \theta_f) \exp(-k_u t)$, where θ_t is the ellipticity measured at time t, θ_f is the final ellipticity value, θ_0 represents the corresponding value at zero time, and k_u is the unfolding rate constant. The kinetics of TIM denaturation was also monitored by changes in near-UV CD (285 nm); in this case, larger volumes of concentrated TIM solution had to be injected to reach a final concentration (ca. 0.5 mg mL^{-1}) appropriate for detection of the ellipticity. Thermal reequilibration in the cell was reached in approximately 40 s.

Refolding Kinetics. The kinetics of TIM refolding was studied by means of CD at 220 nm. A 1.0 cm cell containing 2.700−2.860 mL of the Tris buffer was equilibrated to the temperature of the experiment. Then 140−300 μL of thermally unfolded TIM (a solution of TIM, not exceeding 0.150 mg mL^{-1}, that was heated for 3.0 min at 63.7 °C; see Results) was added to the cell. Thermal equilibration to ±0.15 °C of the setting temperature took approximately 20−30 s. In this way, refolding could be studied in the 0.007−0.015 mg mL^{-1} concentration range. For higher TIM concentrations a second method proved to be more appropriate: TIM was first denatured at 63.7 °C, as in a typical experiment for measuring the kinetics of denaturation. The temperature of the Peltier cell holder was then set to a value 1.0−1.5 °C below that desired for the study of the refolding reaction; this allowed a fast cooling (approximately 15 °C min^{-1}) of the TIM solution. When the temperature in the cell was 0.5 °C above the desired value, the setting was raised to its final value. Inside the cell, temperature oscillations decreased below ±0.2 °C of its final value in approximately 1 min. This method was only used under refolding conditions where the reaction half-life was longer than 4 min. Kinetic data were adjusted to a second-order-reaction equation, $\theta_t = \theta_f + (\theta_0 - \theta_f)/(2C_0k_rt + 1)$, where C_0 is the initial molar concentration of TIM monomers, k_r is the refolding rate constant, and the other parameters have similar meanings as those described above for the single exponential decay equation.

Fluorescence Spectroscopy. Fluorescence spectroscopy experiments were made in a PC1 spectrofluorometer from ISS (Champaign, IL). This instrument was equipped with a water-jacketed cell holder for temperature control. For spectral recordings, samples in a 1.0 cm cell were excited at 290 nm, and emission was collected from 300 to 400 nm. Kinetic experiments were carried out with excitation at 290 nm and emission at 318 nm. The experiments were started by diluting the sample in the same way as described for CD; stirring was also used, and the dead time in this case was approximately 35 s. The temperature was registered using a 5611 thermistor probe connected to a 1504 Hart digital thermometer (Hart Scientific, American Fork, UT) whose calibration is traceable to the National Institute of Standards and Technology. All other temperature probes were calibrated against the Hart instrument.

Changes in Accessible Surface Area. The changes in accessible surface area upon unfolding were estimated from the difference between the native dimer (PDB file 7TIM) and the fully extended chains. All carbon and sulfur atoms were considered to be apolar; nitrogen and oxygen were considered as polar atoms. Area calculations were performed by means of the program NACCESS (Simon Hubbard, University College, United Kingdom), an implementation of the Lee and Richards algorithm (*15*), using a probe radius of 1.4 Å and a slab width of 0.05 Å.

RESULTS

Thermal Transitions of TIM Denaturation and Renaturation. The thermal denaturation and renaturation of TIM were followed by continuous monitoring of the ellipticity at 220 nm at constant heating or cooling rates. Figure 1 shows results obtained with TIM solutions of 0.010 mg mL^{-1} in Tris buffer, pH 8.5 at 25 °C. When temperature was varied at 2.0 °C min^{-1}, an almost perfect hysteresis cycle was observed. After renaturation, the far-UV CD spectrum was essentially identical to that of native TIM, and the recovery of enzymatic activity was larger than 95%. For the sake of comparison, thermal transitions of hen lysozyme (pH 2.5) were registered at the same scanning rate; in this case, denaturation and renaturation profiles were practically superimposable on each other. TIM samples subjected to repetitive denaturation−renaturation cycles exhibited similar hysteresis behavior, but the amount of refolded enzyme decreased after each cycle. Thermal scannings of the protein were also made using Tris buffers covering the pH interval from 7.2 to 9.1 (pH adjusted at 25 °C) and in acidic media (pH 2.0, 3.9, and 4.5). In all of these cases, the reversibility of the denaturation process was significantly less than that attained at pH 8.5. However, the temperature at the middle of the denaturation transition showed only a slight variation within the pH range 7.2−9.1. Kinetic studies were thus carried out with the buffer of pH 8.5. It should be mentioned that aging of the enzyme had detrimental effects on its refolding capacity. In samples stored for a period of 4 months, reversibility decreased to approximately 90%. After 1 year of storage, the enzyme was completely unable to refold. In contrast, aging had only a minor effect on catalytic and spectroscopic characteristics of native TIM, as well as on its thermal denaturation profile.

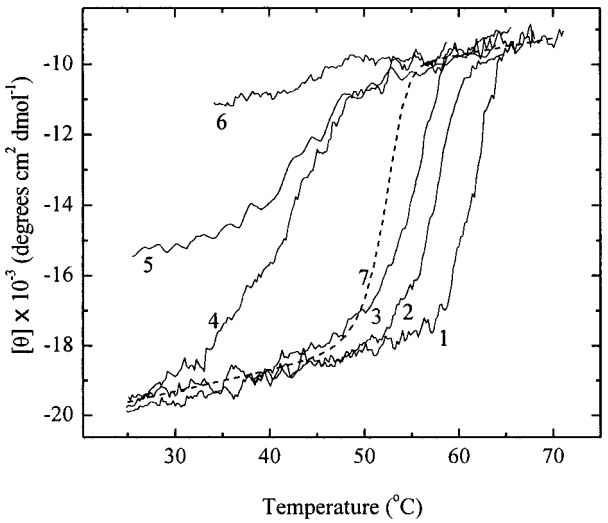

FIGURE 1: Thermal denaturation and renaturation transitions of yeast TIM at pH 8.5. Transition profiles were obtained at different heating and cooling rates as indicated: curves 1 and 4, 2 °C min^{-1}; curves 2 and 5, 0.2 °C min^{-1}; and curves 3 and 6, 0.05 °C min^{-1}. Transitions were monitored by recording the ellipticity at 220 nm. Protein concentration was 0.010 mg mL^{-1}. The dashed line (curve 7) represents a hypothetical equilibrium transition calculated on the assumption of a two-state model (see the text).

As can be seen in Figure 1, decreasing the heating rate in thermal scannings displaced the transition to lower temperature, which is a typical finding in transitions under kinetic control (*16*−*18*). However, smaller heating rates also lead to pronounced irreversibility on the renaturation profile; at scanning rates below 0.2 °C min^{-1} denaturation was completely irreversible as judged by the ellipticity signal. This suggests that the appearance of irreversibility is linked to the residence time of TIM at moderate to high temperatures. Whichever the origin of irreversibility-causing reactions in

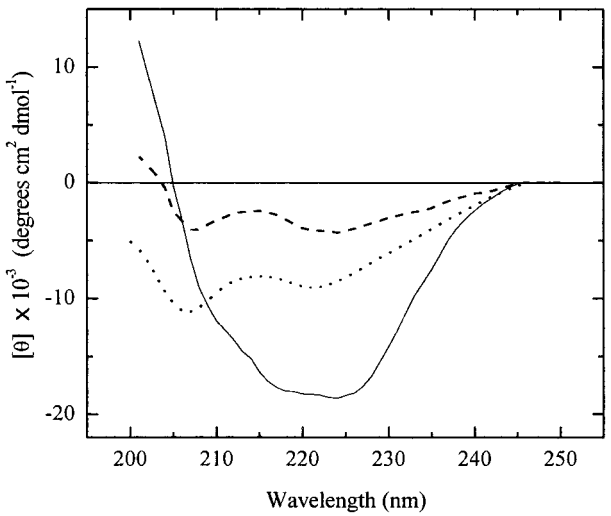

FIGURE 2: Far-UV CD spectra of yeast TIM. Spectra were recorded in 50 mM Tris-HCl buffer (pH 8.5). Native enzyme at 25 °C (solid line); thermally denatured enzyme at 75 °C (dotted line). Also shown is a difference CD curve obtained by subtracting the spectrum of thermally unfolded lysozyme from that of thermally denatured TIM (dashed line).

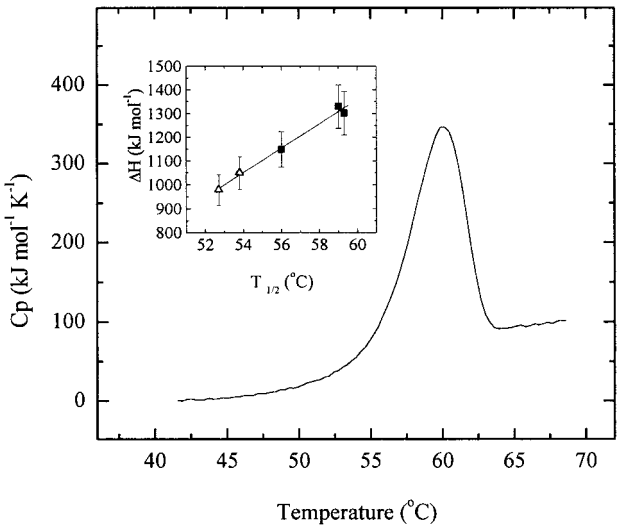

FIGURE 3: DSC curve of yeast TIM after subtraction of a buffer−buffer baseline. The scanning rate was 1 °C min^{-1}, and the protein concentration was 2.27 mg mL^{-1} (pH 8.5). Shown in the inset is the dependence of the enthalpy change on the temperature of half-denaturation, $T_{1/2}$. Measurements were carried out at pH 8.5 (■) and pH 10.0 (△).

yeast TIM, it is clear that these reactions do not affect the far-UV CD of denatured TIM, as indicated by the coincident [θ] values in the postdenaturation region for the different transitions depicted in Figure 1. Linear extrapolations of [θ] values outside the transition regions were used to estimate the expected initial and final ellipticities in kinetic experiments carried out at constant temperature (see below).

Far-UV CD spectra of native and thermally denatured TIM are shown in Figure 2. Although the observed spectral differences are clearly a reflection of important changes in secondary structure of the protein, the spectrum of denatured TIM is not typical of heat-denatured proteins. Indeed, it has been noted that several small monomeric proteins display a common spectral shape upon thermal denaturation (ref *19* and references cited therein), which is characterized by a broad shoulder around 220 nm and a large negative peak at ca. 200 nm. Among these examples it is the case of heat-denatured lysozyme, which is regarded as a completely unfolded protein from the thermodynamic point of view (*20*). Subtraction of the heat-denatured lysozyme spectrum from that of denatured TIM resulted in a difference curve (dashed line in Figure 2) whose shape strongly suggests that a significant amount of secondary structure (over and above that which might exist in a typical thermally unfolded protein) is still present in the thermally denatured isomerase. Such a residual structure might well include about 10% of α-helix and 20% of β-strands, according to the analysis of the difference spectrum by means of the SELCON algorithm (*21*).

Calorimetry of TIM Thermal Denaturation. A DSC recording of the thermal denaturation of TIM (concentration of 2.27 mg mL^{-1}, heating rate of 1 °C min^{-1}) is shown in Figure 3; the thermogram consists of a single, markedly asymmetric endotherm with a maximum point at 60.3 °C. For this particular experiment, $T_{1/2}$ (i.e., the temperature at which the process is half-completed on the basis of the absorbed heat) was determined as 59.5 °C. Experiments were done at various protein concentrations in the range from 0.73 to 2.27 mg mL^{-1}. No significant concentration dependence of $T_{1/2}$ was observed. The average $T_{1/2}$ (59.1 ± 0.4 °C) was very similar to that determined from CD transitions at low TIM concentrations and the same heating rate. In all cases, calorimetric transitions were found to be irreversible as indicated by the absence of the endothermic effect on a second scanning of the sample. Furthermore, samples extracted from the calorimeter after a first scan showed evident aggregation which was more appreciable at high protein concentration.

Despite the irreversible character of TIM denaturation in DSC experiments, the calorimetric enthalpy (ΔH_{cal}) could still be a trustful thermodynamic parameter, provided that exothermic effects from aggregation were not very large (*22*, *23*). Values of ΔH_{cal} obtained from six independent experiments were rather insensitive to variation in protein concentration, suggesting that heat effects from aggregation are not significant. The average ΔH_{cal} was 1330 ± 100 kJ mol^{-1}, which corresponds to 2.7 kJ/mol of amino acid residue. This value is close to the normalized denaturation enthalpies for a number of globular proteins (*24*), whose average at 60 °C amounts to 3.2 ± 0.4 kJ/mol of residue. Therefore, according to this thermodynamic criterion heat-denatured TIM seems to be extensively unfolded.

Additional experiments showed that $T_{1/2}$ decreased as the scanning rate was reduced, in agreement with results mentioned above. Besides, determinations of ΔH_{cal} from these endotherms, complemented with some measurements carried out at pH 10.0, were used to construct a plot of ΔH_{cal} vs $T_{1/2}$ (inset to Figure 3). It is generally accepted that the temperature dependence of ΔH_{cal} can be described by a linear function whose slope equals the molar heat capacity difference between unfolded and native states, ΔC_p (*20*, *25*). Thus, from the straight line drawn in Figure 3, ΔC_p was estimated as 49 ± 3 kJ mol^{-1} K^{-1}. If it is assumed that denaturation involves dissociation and complete unfolding of monomers, the expected ΔC_p [calculated from changes in polar and apolar accessible surface areas according to well-known parametrized equations (*24*, *26*)] would be between 35 and

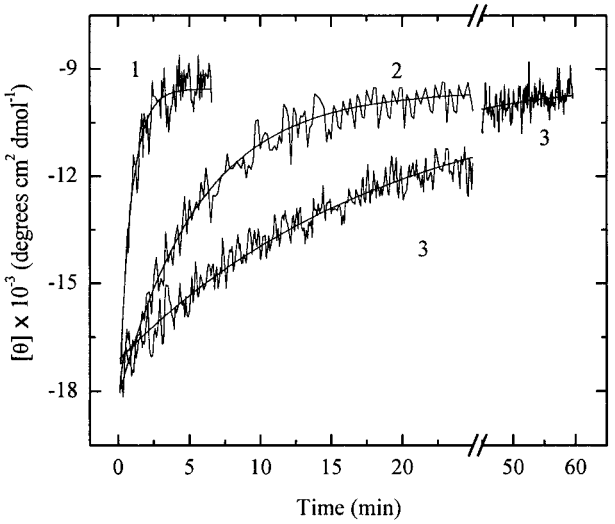

FIGURE 4: Kinetics of thermal denaturation of yeast TIM at different temperatures followed by CD spectroscopy at 220 nm. Data shown correspond to the following temperatures: 62.8 (curve 1), 57.8 (curve 2), and 52.4 °C (curve 3). Smooth lines are single exponential decay curves fitted to experimental data. Protein concentration was 0.010 mg mL^{-1}.

46 kJ mol^{-1} K^{-1}, in reasonable agreement with the experimental estimation. It must be mentioned that TIM endotherms showed the expected increase in heat capacity upon denaturation (Figure 3); however, quantitative determinations of ΔC_p from the pre- and postdenaturation heat capacities of different endotherms gave such a variability that a meaningful estimation of ΔC_p could not be obtained.

Denaturation Kinetics. The time course of TIM unfolding at constant temperature was followed by changes in ellipticity at 220 nm, which report on the loss of secondary structure. Figure 4 shows results obtained at different temperatures. In all cases, single exponential decay curves fitted well the experimental data. Ellipticity values extrapolated to time zero were very similar to those expected for the native protein, indicating that no significant structural changes occur in a fast kinetic phase that might have been lost during the dead time of experiments. In the range from 0.010 to 0.060 mg mL^{-1}, protein concentration had practically no effect on the rate constant, stressing the fact that TIM denaturation follows simple first-order kinetics. A salient feature of the denaturation curves is that all of them reach similar final $[\theta]$ values; that is, the reaction proceeds to completion as an irreversible reaction does. However, at high temperatures (greater than 63 °C), when TIM unfolding does not take long times, the process was found to be completely reversible. For instance, at 63.7 °C the loss of secondary structure occurs rapidly (in 3.0 min the reaction is more than 98% complete as indicated by the ellipticity), yet the native structure is fully recovered when the protein is quickly cooled (15 °C min^{-1}) to 25 °C. For longer periods of TIM incubation at high temperature no further changes in CD signal are observed, but the refolding capacity decreases notably. This indicates that the main source of irreversibility resides in reactions that occur after TIM unfolding but are silent about far-UV CD.

Changes in tertiary interactions during TIM denaturation were followed by monitoring the ellipticity at 285 nm on protein solutions of 0.5 mg mL^{-1}. Experiments were conducted at 55.2 and 58.5 °C. At the highest temperature the observed kinetic curves were distinctly biphasic (results not shown). Curve fitting according to a double exponential decay model gave an amplitude of 68−72% (relative to the total change in ellipticity) for the fast kinetic phase; the value of the rate constant for this phase was the same (within experimental error) as that determined from far-UV measurements at the same temperature. The slow phase, which was accompanied by the appearance of turbidity in the TIM solution, had a rate constant approximately 13 times smaller than that for the fast phase. In contrast, at 55.2 °C the loss of near-UV ellipticity followed a simple exponential decay model. A single kinetic phase, whose rate constant was again identical to the one determined from the loss of secondary structure, accounted for the total change in $[\theta]_{285}$ and was associated with sample turbidity.

Further characterization of TIM denaturation was achieved by means of fluorescence measurements. These studies were aimed at detecting changes of polarity in the environment of tryptophan residues, which are thought to be reflected in spectral red shifts. A series of emission spectra were recorded at intervals of 540 s during the course of TIM denaturation at 56.8 °C. Spectra shown in Figure 5a are representative of the changes that took place. The absence of an isofluorescent point in these curves indicates that more than two species are involved in the process. Furthermore, two distinct trends are easily discerned. Spectra corresponding to reaction times up to 45 min are progressively red shifted from 320 to 328 nm and display an important loss of intensity at shorter wavelengths. Further red shifts and increasing intensities at longer wavelengths typify the spectral changes for late reaction times. In concordance with this observation, kinetic plots constructed from the intensities measured at a particular wavelength exhibited a distinctive biphasic character; however, the distinction between the two phases was most evident at 318 nm. Hence, the latter emission wavelength was chosen for kinetic measurements at other temperatures (Figure 5b). At all temperatures tested (54.9−61.8 °C), data fitting to a double exponential decay equation gave a value for the largest rate constant that was close, if not identical, to that for the rate constant determined from CD.

According to the above results, the kinetics of TIM denaturation can be described as a sequential pathway whose first step leads to the simultaneous loss of most of the tertiary interactions and a considerable part of the secondary structure of the molecule. This unfolding step also involves an increase in the polarity of tryptophyl surroundings. Subsequent reactions entail no further changes in secondary structure but apparently cause further changes in the environment of tryptophan residues. Besides, these late reactions bring the unfolded protein to a state that is irreversibly denatured. At high protein concentration (0.5 mg mL^{-1}), irreversibility is clearly linked to the formation of large molecular aggregates.

Temperature Dependence of the Unfolding Rate Constant. The effect of temperature on the rate constant for the unfolding step of TIM denaturation (k_u) is illustrated in Figure 6. The plotting of $\ln(k_u/T)$ vs $1/T$ conforms to the well-known Eyring's equation:

$$\ln(k/T) = \ln E + \Delta S^{\ddagger}/R - (\Delta H^{\ddagger}/R)(1/T) \qquad (1)$$

where k is the rate constant of an elementary reaction; E represents a preexponential factor, which in Eyring's formulation is equal to the ratio of Boltzmann's constant to

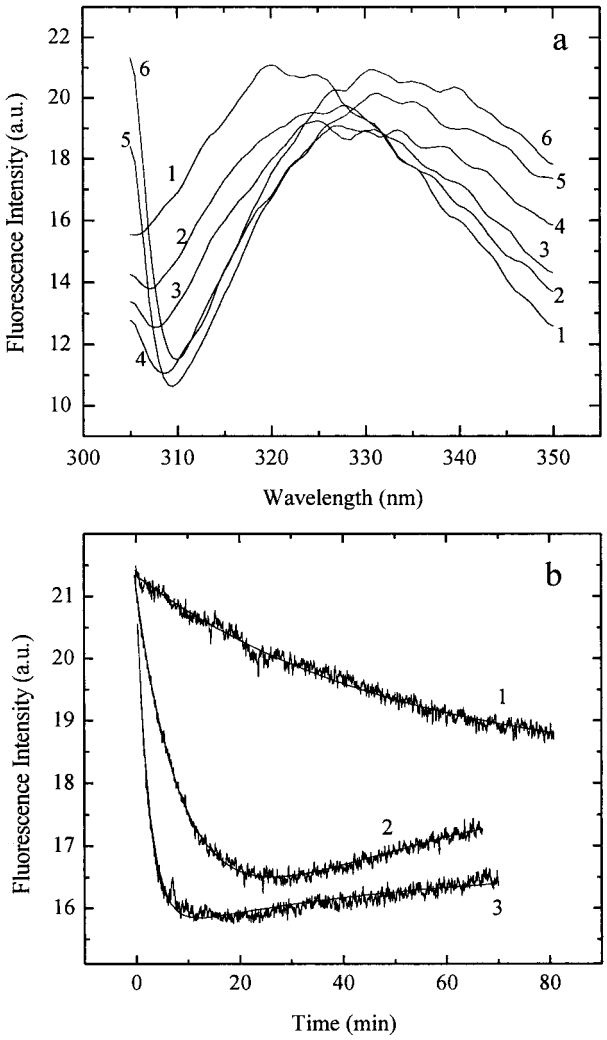

FIGURE 5: Thermal denaturation of yeast TIM monitored by fluorescence spectroscopy. Panel a shows emission spectra (samples were excited at 290 nm) recorded at several times after the start of the reaction at 56.8 °C: 0.7 (curve 1), 9 (curve 2), 18 (curve 3), 36 (curve 4), 126 (curve 5), and 216 min (curve 6). Panel b shows kinetic curves monitored by recording the emission at 318 nm. Data shown correspond to the following temperatures: 54.9 (curve 1), 59.8 (curve 2), and 61.8 °C (curve 3). Data points were fitted to biphasic exponential decay curves (smooth lines). Protein concentration was 0.050 mg mL^{-1}.

Planck's constant; $\Delta H^{\ddagger}$ and $\Delta S^{\ddagger}$ are the activation enthalpy and entropy, respectively. When the variation of $\Delta H^{\ddagger}$ and $\Delta S^{\ddagger}$ with temperature is explicitly taken into account, eq 1 transforms to (*27*)

$$\ln(k/T) = A - B(1/T) - (\Delta C_p^{\ddagger}/R)\ln(1/T) \qquad (2)$$

where the activation heat capacity, $\Delta C_p^{\ddagger}$, is assumed to be temperature independent. Coefficients A and B are expressed as combinations of activation parameters; here we used the form $A = \ln E + (\Delta S_r^{\ddagger} - \Delta C_p^{\ddagger} - \Delta C_p^{\ddagger} \ln T_r)/R$ and $B = (\Delta H^{\ddagger}_{T_r} - \Delta C_p^{\ddagger} T_r)/R$, which allows for an easy calculation of $\Delta H^{\ddagger}$ at any particular temperature, T_r, chosen as reference.

Analysis of unfolding data in Figure 6 according to eq 2 gave a $\Delta C_p^{\ddagger}{}_u$ of 2.1 ± 5.9 kJ mol^{-1} K^{-1}. In comparison with the calorimetric ΔC_p (49 ± 3 kJ mol^{-1} K^{-1}), $\Delta C_p^{\ddagger}{}_u$ turns out to be certainly small if not negligible at all. This finding is in agreement with previous studies on the unfolding of

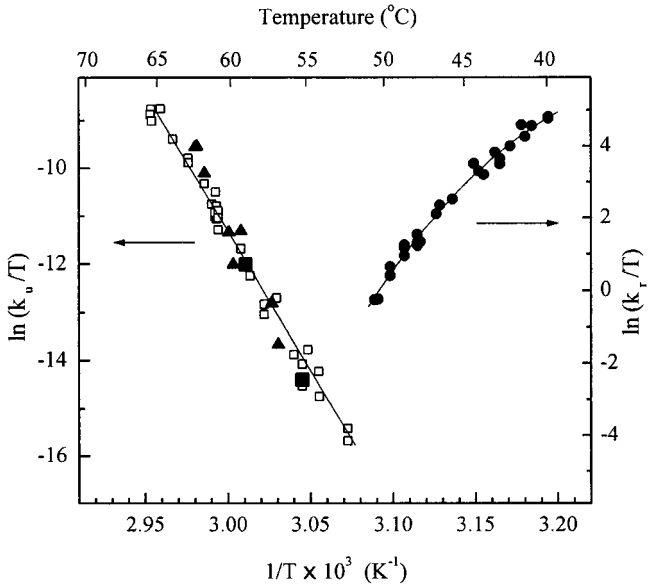

FIGURE 6: Eyring's plots for the rate constants of unfolding (k_u) and refolding (k_r) of yeast TIM. Denaturation data were obtained by means of far-UV CD (□), near-UV CD (■), and fluorescence spectroscopy (▲). Refolding rate constants (●) were determined from far-UV CD measurements. Lines shown are least-squares regressions according to eq 1 (unfolding) or eq 2 (refolding): $\ln(k_u/T) = 162\ (\pm 4) - 57\,900\ (\pm 1500)\ (1/T)$; $\ln(k_r/T) = 25\,500\ (\pm 5500) - 1.16 \times 10^6\ (\pm 0.26 \times 10^6)\ (1/T) + 3800\ (\pm 800)\ (\ln(1/T))$; k_u and k_r are given in s^{-1} and M^{-1} s^{-1}, respectively.

monomeric proteins in aqueous solution (*19*, *28*−*32*), where linear or nearly linear plots of $\ln(k_u/T)$ vs $1/T$ have been reported. Fitting of unfolding data to the linear model (eq 1) gave a $\Delta H^{\ddagger}_u$ of 480 kJ mol^{-1}. In comparison, values of $\Delta H^{\ddagger}_u$ for monomeric proteins are comprised in the interval from 100 to 350 kJ mol^{-1} (ref *33* and references cited therein).

Renaturation Kinetics. The recovery of secondary structure upon TIM renaturation was followed by monitoring of the ellipticity at 220 nm. The starting material in these studies was a solution of TIM (not exceeding 0.150 mg mL^{-1}) previously denatured for 3 min at 63.7 °C. As mentioned above, these denaturing conditions ensured the formation of a reversibly unfolded state. Refolding experiments were started by either of the two thermal equilibration approaches described in Materials and Methods.

Figure 7 shows two kinetic curves, recorded at 48.3 °C, corresponding to different TIM concentrations. Both curves in this figure reach a $[\theta]$ value close to that for native TIM at the same temperature (as deduced from the predenaturation region in Figure 1), thus indicating that refolding is almost complete in these conditions. Besides, it is evident that the reaction half-life decreases with protein concentration. Several refolding experiments were done in the range from 0.007 to 0.040 mg mL^{-1}; the observed half-life times ($t_{1/2}$) are plotted against the reciprocal of the molar concentration of TIM monomers in Figure 8. Despite experimental error, the evident linearity of this plot is consistent with the relationship expected for a second-order reaction: $t_{1/2} = 1/(2C_0k_r)$, where k_r is the rate constant, and C_0 is the initial monomer concentration. Furthermore, the value of k_r calculated from the line in Figure 8 ($1.5 \times 10^3 \pm 0.1 \times 10^3$ M^{-1} s^{-1}) was in excellent agreement with the average k_r ($1.4 \times 10^3 \pm 0.5 \times 10^3$ M^{-1} s^{-1}) obtained by fitting individual

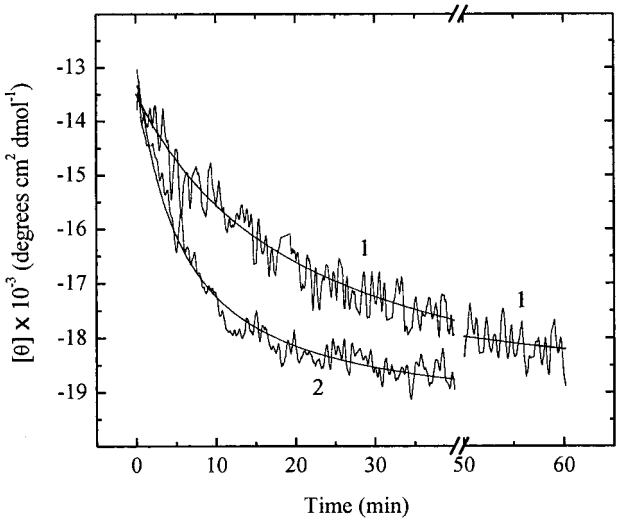

FIGURE 7: Time course of yeast TIM refolding at 48.3 °C and two different protein concentrations. Refolding was followed by changes in ellipticity at 220 nm. Data shown correspond to 0.007 mg mL^{-1} (curve 1) and 0.040 mg mL^{-1} (curve 2). Data points were fitted to a single second-order reaction (smooth lines).

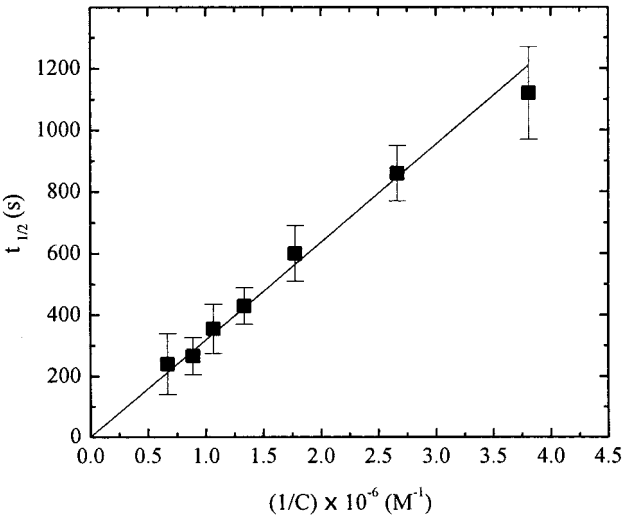

FIGURE 8: Effect of protein concentration on the half-life of TIM refolding. Experiments were carried out at 48.3 ± 0.2 °C with TIM samples of 0.007−0.040 mg mL^{-1}. Concentration is expressed in terms of monomer molarity (M_r = 26 650).

experimental curves to second-order kinetics. Similar dependence of $t_{1/2}$ on protein concentration was observed at 43.2 °C (results not shown).

TIM refolded under the conditions described above showed more than 95% recovery of enzymatic activity when assayed in standard conditions (pH 7.4, 25 °C). Reactivation was also investigated in refolding conditions (pH 8.5, 43.2 °C). Assays made with TIM samples in which refolding had advanced approximately 95% indicated that activity had also been recovered to a good extent (more than 90% with respect to native TIM assayed in identical conditions). A thorough study of activity regain during renaturation was, however, not feasible because the substrate seemed to promote reactivation. Indeed, it was observed that when transferred to assay conditions, unfolded TIM initially displayed zero enzymatic activity, but the activity increased during the time of the assay (i.e., large curvature was observed in the tracings of absorbance changes).

Temperature Dependence of the Refolding Rate Constant. Determinations of k_r were made in the interval from 40 to 51 °C. In most experiments, the total protein concentration was 0.010 mg mL^{-1}; however, in determinations carried out above 48 °C the concentration was increased (0.030−0.040 mg mL^{-1}) to reduce the time required for refolding, thus avoiding the appearance of irreversibly denatured species. In all cases, k_r was determined from experiments in which refolding was more than 95% complete. Results are shown in the corresponding Eyring's plot of Figure 6. The evident downward curvature there observed, akin to that found in analogous plots for the refolding of monomeric proteins (*28*−*31*) or for the association−refolding reaction of the small P22 Arc repressor (*34*), is consistent with a negative ΔC_p of activation. Least-squares fitting of eq 2 to k_r data gave the set of parameters shown in the legend to Figure 6; the corresponding value of $\Delta C_p^{\ddagger}{}_r$ is -31 ± 7 kJ mol^{-1} K^{-1}.

DISCUSSION

As has been found for several TIM enzymes, thermal denaturation of yeast TIM is highly irreversible under a number of conditions. Yet, at pH 8.5 and low protein concentration complete unfolding−refolding transitions were observed by thermal scanning at rates above 1.0 °C min^{-1}. In these circumstances, the two transitions are completely separated from each other, suggesting that slow kinetic events prevent the reaching of equilibrium during heating and cooling cycles. Attempts to approach equilibrium by scanning at lower rates are of no help because the process becomes irreversible.

Results from our study of the kinetics of TIM denaturation indicate that irreversibility originates from reactions taking place after an initial unfolding step. Most probably, aggregation of the thermally unfolded protein can be regarded as the main cause of irreversibility, as it is frequently observed with oligomeric proteins (*35*). The first step in the denaturation pathway obeys simple first-order kinetics, pointing out its unimolecular nature. This reaction results in the formation of what we have called *thermally unfolded*, U, TIM which can be described as a molecular form lacking most of the tertiary interactions present in native, N, TIM. Furthermore, extensive regions of the native molecule seemingly become exposed to the solvent in the U species, as inferred from the large ΔC_p of denaturation. Also, tryptophan residues appear to be more exposed to the solvent in U than in N. On the other hand, U apparently possesses significant secondary structure (including, perhaps, some helical and β-strand regions) as its far-UV CD spectrum indicates. Nevertheless, on account of the relatively high enthalpy of denaturation on a per residue basis, it seems unlikely that the structural elements remaining in U be associated into a large cooperatively folded unit, at least as far as enthalpy changes are regarded (*24*, *36*). Notwithstanding the propensity of U to aggregate, it was found that at temperatures above 63 °C and low TIM concentration (less than 0.150 mg mL^{-1}) the time span for the unfolding reaction was much shorter than that for the reactions leading to irreversibility. This allowed us to demonstrate that unfolded TIM is fully able to refold trough a second-order reaction that produces nativelike dimeric TIM, thus indicating the monomeric character of the U species.

Table 1: Calorimetric and Activation Parameters That Characterize TIM Unfolding and Refolding[a]

	enthalpy (kJ mol^{-1})				molar heat capacity (kJ mol^{-1} K^{-1})		
temp (°C)	$\Delta H^{\ddagger}_{u}$	$\Delta H^{\ddagger}_{r}$	$\Delta H^{\ddagger}_{u} - \Delta H^{\ddagger}_{r}$	ΔH_{cal}	$\Delta C_p^{\ddagger}{}_{u}$	$\Delta C_p^{\ddagger}{}_{r}$	$\Delta C_{p\,cal}$
49.0	480 (10)	−510 (30)	990 (30)	810[b] (50)	≈0	−31 (7)	49 (3)
53.8	480 (10)	−660 (60)	1140 (60)	1050 (70)			
59.0	480 (10)	−830 (90)	1310 (90)	1330 (100)			

[a] Activation parameters were calculated from the least-squares regressions shown in the legend to Figure 6. The calorimetric enthalpy was measured directly from DSC scannings. $\Delta C_{p\,cal}$ was calculated from the slope of the line shown in the inset to Figure 3. Standard deviations are indicated in parentheses. [b] Value extrapolated from the line shown in the inset to Figure 3.

The kinetics of refolding was studied over a temperature range where the reaction was essentially irreversible and its rate constant (k_r) accurately measurable. The temperature dependence of k_r was found to be consistent with a large negative $\Delta C_p^{\ddagger}{}_{r}$, resembling in this regard the refolding kinetics of monomeric proteins (*28*−*31*). According to the curve drawn in Figure 6, around 30 °C k_r would reach its maximum value of 1.8×10^5 M^{-1} s^{-1}. Interestingly, this magnitude is comparable to those reported before for the rate constant of the association step (k_{bi}) in the renaturation of GuHCl-unfolded TIM: for rabbit muscle TIM (pH 7.5, 0.065 M GuHCl) k_{bi} equals 3×10^5 M^{-1} s^{-1} at 0 °C (*4*); in the case of the enzyme from chicken muscle (pH 7.5, 0.40 M GuHCl) k_{bi} is approximately 2.2×10^4 M^{-1} s^{-1} near 30 °C (*37*). It should be noted, however, that renaturation of TIM from its GuHCl-unfolded monomers conforms adequately to a sequential uni-bimolecular kinetic mechanism: unfolded monomer → intermediate monomer → native dimer, where the intermediate has been referred to as a "folded" or compact monomer (*4*, *38-40*). Nevertheless, because the regain of secondary structure during renaturation has not been addressed by previous studies, the degree of structural organization attained in the intermediate cannot be assessed to date. In this regard, recent studies (*5*, *6*) on the denaturation of yeast TIM induced by GuHCl have shown that a partially folded monomer is well populated at moderate denaturant concentration (i.e., about 1.0 M; pH near neutrality). This intermediate lacks persistent tertiary interactions but possesses residual secondary structure as judged from its far-UV CD spectrum (*6*). It remains to be demonstrated whether a similar partially folded monomer appears as a kinetic intermediate in the formation of dimeric TIM under conditions strongly favoring the native state; yet, Morgan et al. (*6*) have advanced the idea that this could be so. Such a proposal is now strongly supported in view of the structural resemblance of the last mentioned intermediate to the *thermally unfolded* monomer which, as shown in the present work, is fully competent for dimerization. Thus, near physiological conditions the renaturation of yeast TIM from its highly unstructured monomers (i.e., as they occur in high concentration of denaturant) might likely involve two major folding steps: The first is the fast formation of a framework intermediate structurally similar to the *thermally unfolded* monomer. In this step, the appearance of some secondary structure elements would be induced by the fast collapse of the polypeptide chain brought about by the change in solvent conditions; as our observations imply, such a structural scaffolding is stable in the absence of denaturant, suffering only gradual changes as the temperature is risen up to 75 °C. The second is the association step leading to formation of the dimer, with the concomitant regain of the rest of the secondary structure and the burial of large amounts of solvent-accessible surface area. Probably, most of the native tertiary interactions would also be established during this step, although the occurrence of subsequent rearrangements necessary for the development of enzymatic activity cannot be ruled out.

Even though the thermal unfolding of yeast TIM is a reversible process, the study of its kinetics and equilibrium properties, in conditions where both N and U are expected to be appreciably populated at equilibrium, is precluded by the tendency of the latter species toward forming irreversibly denatured aggregates, together with the apparent slowness of the unfolding reaction. Therefore, it is impossible to ascertain whether stable intermediates coexist in equilibrium with N and U within a particular temperature range. Nevertheless, our results from studies of the refolding and unfolding kinetics suggest that a simple two-state model may give a reasonable description of the unfolding equilibrium:

$$N \underset{k_r}{\overset{k_u}{\rightleftarrows}} 2U \qquad (3)$$

Additional evidence in favor of this model must be sought in the comparison of the calorimetric ΔC_p and ΔH (regarded as descriptors of the global process) with the corresponding activation parameters. Both sets of parameters are summarized in Table 1. For the two-state model to be valid, the approximation $\Delta C_{p\,cal} \approx -\Delta C_p^{\ddagger}{}_{r}$ must hold because $\Delta C_p^{\ddagger}{}_{u}$ is negligibly small. However, the value of 49 kJ mol^{-1} K^{-1} for $\Delta C_{p\,cal}$ lies outside the 95% confidence interval for $-\Delta C_p^{\ddagger}{}_{r}$ (31 ± 13 kJ mol^{-1} K^{-1}; calculated from its standard error in the regression to eq 2), indicating that the difference in heat capacities may be significant. Likewise, the sum of $\Delta H^{\ddagger}_{u}$ and $-\Delta H^{\ddagger}_{r}$ significantly exceeds the (extrapolated) value of ΔH_{cal} at low temperature, although above 53 °C both estimators of the global unfolding enthalpy are in excellent agreement (Table 1). The discrepancies just noted may indicate the existence of an intermediate state between N and U or that unfolding and refolding reactions follow different pathways. Nevertheless, it is possible that the lack of agreement between calorimetric and kinetic results had originated from an overestimation of $\Delta C_{p\,cal}$ due to aggregation. Indeed, a small exothermic effect may have little influence on ΔH_{cal} at a given temperature; yet if the magnitude of this effect decreases with temperature, the apparent $\Delta C_{p\,cal}$ (as measured from the slope of a plot of ΔH_{cal} vs $T_{1/2}$) would be larger than the real ΔC_p for the unfolding transition.

Evaluation of the Thermodynamic Stability from a Putative Two-State Model. Although it cannot be conclusively established whether the thermal unfolding of yeast TIM conforms to a two-state model, for dimeric human TIM the validity of such a model has received partial support from fluores-

cence studies of its thermal unfolding equilibrium (*12*). It is thus interesting to estimate the stability of yeast TIM on the assumption of the two-state model in order to compare such results with those reported for the human enzyme. Accordingly, the equilibrium constant for the unfolding of yeast TIM can be obtained from the relationship:

$$K_u = k_u/k_r \quad (4)$$

On the other hand, K_u is related to the fraction of unfolded protein, f_u, by the equation:

$$K_u = 2C_t[f_u^2/(1 - f_u)] \quad (5)$$

where C_t is the total protein concentration expressed in terms of monomers. Because the temperature dependences of k_u and k_r are known, eqs 4 and 5 can be used to calculate f_u as a function of temperature. For a protein concentration of 0.010 mg mL^{-1}, the calculated transition curve (dotted line in Figure 1) displays a temperature of half-denaturation ($T_{1/2}$) of 51.8 °C, which is similar to that reported for human TIM (approximately 54 °C) at pH 8.0 and the same protein concentration (*12*). Values of K_u from eq 4 were also used to estimate the standard free energy change ($\Delta G_u = -RT \ln K_u$) for the unfolding process of yeast TIM. The maximum value of ΔG_u (90 kJ mol^{-1}) is expected to occur around 21 °C. For human TIM, ΔG_u has been estimated as 80.7 kJ mol^{-1} (19.3 kcal mol^{-1}) at 25 °C. The agreement in ΔG_u, however, seems to be rather fortuitous, for there is a large discrepancy between the $\Delta C_{p\,u}$ of 31 kJ mol^{-1} K^{-1} used in our calculations (i.e., $\Delta C_{p\,u}$ was approximated as $-\Delta C_p^{\ddagger}{}_r$) and the small value of 6.3 kJ mol^{-1} K^{-1} estimated by Mainfroid et al. (*12*) from the variation of ΔH_u with $T_{1/2}$. It should be noted that these authors determined ΔH_u by van't Hoff analysis of fluorescence-detected transitions; unfortunately, no values of ΔH_u were reported. Clearly, further studies are needed to accurately establish the thermodynamic properties of this family of dimeric enzymes.

A final point that deserves comment refers to the hysteresis displayed in the thermal scannings of TIM (Figure 1), an observation that contrasts with the behavior of small monomeric proteins whose thermal transitions recorded at 1 or 2 °C/min are usually close to the true equilibrium curve. The simplest explanation for such a distinct behavior is that within the transition region the unfolding−refolding kinetics of TIM is much slower than that for a typical monomeric protein. For example, at the temperature of half-denaturation the value of the unfolding and refolding rate constants for lysozyme (*29*) ranges from 0.05 to 0.90 s^{-1}, depending on the pH. This means that upon a temperature perturbation the populations of folded and unfolded molecules would approach their equilibrium values with a relaxation time [$\tau = 1/(k_u + k_r)$] of 0.5−10 s. Even for the larger bovine trypsin (*28*) τ is expected to be only about 0.5 min at $T_{1/2}$. For a system comprised of native dimers in equilibrium with unfolded monomers the response to a small perturbation is characterized by a relaxation time given by (*41*)

$$\tau = 1/(k_u + 4k_r[U]_e) \quad (6)$$

where $[U]_e$ is the equilibrium concentration of the unfolded monomers before the perturbation is applied. In the TIM case, k_u and k_r evaluated at the putative $T_{1/2}$ (51.8 °C) have values of 4.5 × 10^{-5} s^{-1} and 124 M^{-1} s^{-1}, respectively. Because the expected $[U]_e$ would be 1.87 × 10^{-7} M (for a total protein concentration of 0.010 mg mL^{-1}), the relaxation time under these conditions can be calculated as 120 min, which is more than 200 times longer than the time required for the relaxation of monomeric proteins. Thus, very long incubation times or very low scanning rates would be required to achieve the native dimer−unfolded monomer equilibrium in a TIM sample. Of course, the occurrence of further reactions (such as unspecific aggregation of U) would render the process overall irreversible. Nevertheless, because of the large magnitude of $\Delta H^{\ddagger}_u$, unfolding proceeds rapidly and essentially to completion when the temperature is only a few degrees above $T_{1/2}$. Similarly, refolding is strongly favored, both kinetically and thermodynamically, at temperatures slightly below $T_{1/2}$. Furthermore, these considerations indicate that the thermostability of TIM, regarded as the half-life of the catalytically active dimer, is governed by the kinetic barrier for the unfolding reaction and the temperature dependence of this barrier.

ACKNOWLEDGMENT

We gratefully acknowledge Dr. Alejandro Fernández-Velasco and Mr. Hugo Najera-Peña (Facultad de Medicina, UNAM, México) for their help with the purification of part of the yeast TIM used in this study.

REFERENCES

1. Lolis, E., and Petsko, G. A. (1990) *Biochemistry 29*, 6619−6625.
2. Bränden, C. I. (1991) *Curr. Opin. Struct. Biol. 1*, 978−983.
3. Waley, S. G. (1973) *Biochem. J. 135*, 165−172.
4. Zabori, S., Rudolph, R., and Jaenicke, R. (1980) *Z. Naturforsch. 35c*, 999−1004.
5. Vázquez-Contreras, E., Zubillaga, R. A., Mendoza-Hernández, G., Costas, M., and Fernández-Velasco, A. (2000) *Protein Pept. Lett. 7*, 57−64.
6. Morgan, C. J., Wilkins, D. K., Smith, L. J., Yasushi, K., and Dobson, C. M. (2000) *J. Mol. Biol. 300*, 11−16.
7. Schliebs W., Thanki, N., Eritja, R., and Wierenga, R. K. (1996) *Protein Sci. 5*, 229−239.
8. Schliebs W., Thanki, N., Jaenicke, R., and Wierenga, R. K. (1997) *Biochemistry 36*, 9655−9662.
9. Alvarez, M., Zeelen, J. Ph., Mainfroid, V., Rentier-Delrue, F., Martial, J. A., Wyns, L., Wierenga, R. K., and Maes, D. (1998) *J. Biol. Chem. 273*, 2199−2206.
10. Gopal, B., Ray, S. S., Gokhale, R. S., Balaram, H., Murthy, M. R. N., and Balaram, P. (1999) *Biochemistry 38*, 478−486.
11. Sun, J., and Sampson, N. S. (1999) *Biochemistry 38*, 11474−11481.
12. Mainfroid, V., Terpstra, P., Beauregard, M., Frère, J. M., Mande, S. C., Hol, W. G., Martial, J. A., and Goraj, K. (1996) *J. Mol. Biol. 257*, 441−456.
13. Norton, I. L., and Hartman, F. C. (1972) *Biochemistry 11*, 4435−4441.
14. Rozacky, E. E., Sawyer, T. H., Barton, R. A., and Gracy, R. W. (1971) *Arch. Biochem. Biophys. 146*, 312−320.
15. Lee, B., and Richards, F. M. (1971) *J. Mol. Biol. 55*, 379−400.
16. Freire, E., van Osdol, W. W., Mayorga, O. L., and Sánchez-Ruiz, J. M. (1990) *Annu. Rev. Biophys. Biophys. Chem. 19*, 159−188.
17. Sánchez-Ruiz, J. M. (1992) *Biophys. J. 61*, 921−935.
18. Tello-Solís, S. R., and Hernández-Arana, A. (1995) *Biochem J. 311*, 969−974.
19. López-Arenas, L., Solís-Mendiola, S., and Hernández-Arana, A. (1999) *Biochemistry 38*, 15936−15943.
20. Privalov, P. L. (1979) *Adv. Protein Chem. 33*, 167−241.

21. Sreerama, N., and Woody, R. W. (1993) *Anal. Biochem. 209*, 32−44.
22. Milardi, D., La-Rosa, C., and Grasso, D. (1994) *Biophys. Chem. 52*, 183−189.
23. Goins, B., and Freire, E. (1988) *Biochemistry 27*, 2046−2052.
24. Murphy, K. P., and Freire, E. (1992) *Adv. Protein Chem. 43*, 313−361.
25. Privalov, P. L., and Gill, S. J. (1988) *Adv. Protein Chem. 39*, 191−234.
26. Spolar, R. S., Livingstone, J. R., and Record, T. M., Jr. (1992) *Biochemistry 31*, 3947−3955.
27. Chen, B., Baase, W. A., and Schellman, J. A. (1989) *Biochemistry 28*, 691−699.
28. Pohl, F. M. (1968) *Eur. J. Biochem. 7*, 146−152.
29. Segawa, S. I., and Sugihara, M. (1984) *Biopolymers 23*, 2473−2488.
30. Jackson, S. E., and Fersht, A. R. (1991) *Biochemistry 30*, 10436−10443.
31. Alexander, P., Orban, J., and Bryan, P. (1992) *Biochemistry 31*, 7243−7248.
32. Oliveberg, M., and Fersht, A. R. (1996) *Biochemistry 35*, 2726−2737.
33. Solís-Mendiola, S., Gutiérrez-González, L. H., Arroyo-Reyna, A., Padilla-Zúñiga, J., Rojo-Domínguez, A., and Hernández-Arana, A. (1998) *Biochim. Biophys. Acta 1388*, 363−372.
34. Milla, M. E., and Sauer, R. T. (1994) *Biochemistry 33*, 1125−1133.
35. Garel, J. R. (1992) in *Protein Folding* (Creighton, T. E., Ed.) pp 405−454, W. H. Freeman, New York.
36. Privalov, P. L. (1992) In *Protein Folding* (Creighton, T. E., Ed.) pp 83−126, W. H. Freeman, New York.
37. McVittie, J. D., Esnouf, P., and Peacocke, A. R. (1977) *Eur. J. Biochem. 81*, 307−315.
38. Rietveld, A. W. M., and Ferreira, S. T. (1998) *Biochemistry 37*, 933−937.
39. Gao, X.-G., Garza-Ramos, G., Saavedra-Lira, E., Cabrera, N., Tuena de Gómez-Puyou, M., Pérez-Monfort, R., and Gómez-Puyou, A. (1998) *Biochem. J. 332*, 91−96.
40. Gokhale, R. S., Ray, S. S., Balaram, H., and Balaram, P. (1999) *Biochemistry 38*, 423−431.
41. Nölting, B. (1999) *Protein Folding Kinetics*, pp 44−47, Springer, Berlin.

BI010528W